

# Efficient computation of optical forces with the coupled dipole method

Patrick C. Chaumet

*Institut Fresnel (UMR 6133), Université Paul Cézanne, Avenue Escadrille Normandie-Niemen, F-13397 Marseille Cedex 20, France*

Adel Rahmani

*Laboratoire d'Electronique, Optoélectronique et Microsystèmes (UMR CNRS 5512), Ecole Centrale de Lyon 36, Avenue Guy de Collongue, F-69134 Ecully Cedex, France*

Anne Sentenac

*Institut Fresnel (UMR 6133), Université Paul Cézanne, Avenue Escadrille Normandie-Niemen, F-13397 Marseille Cedex 20, France*

Garnett W. Bryant

*Atomic Physics Division, National Institute of Standards and Technology, Gaithersburg, Maryland 20899-8423, USA*

(Received 30 June 2005; published 18 October 2005)

We present computational techniques to compute in an efficient way optical forces on arbitrary nanoobjects using the coupled dipole method. We show how the time of computation can be reduced by several orders of magnitude with the help of fast-Fourier-transform techniques. We also discuss the influence of different formulations of the electric polarizability of a small scatterer on the accuracy and robustness of the computation of optical forces.

DOI: [10.1103/PhysRevE.72.046708](https://doi.org/10.1103/PhysRevE.72.046708)

PACS number(s): 42.25.Fx, 41.20.-q, 78.20.Bh, 42.25.Bs

## I. INTRODUCTION

Optical forces have become central to many areas of physics and biology, allowing for the cooling and trapping of atoms, the nanomanipulation of biological cells, or the study of biological motors [1]. The mechanical effect of light on matter is also at the core of recent proposals for the observation of quantum superposition and entanglement at the macroscopic level [2]. As optical forces play an increasingly important role in complex systems, it becomes essential to develop efficient numerical techniques to compute optical forces in arbitrary geometries. Several methods have been used to compute electromagnetic forces for an arbitrary object in three dimension such as the multiple multipole method [3], the finite difference in time domain method [4], the  $T$ -matrix method [5], and the coupled dipole method (CDM) [6].

Here we shall consider the CDM. The principle of the method is to discretize the object in subunits smaller than the wavelength of light inside the object. Hence for a large object (compared to the wavelength) the time of computation becomes quickly prohibitive due to the large number of subunits. As the systems of experimental interest are often larger than the wavelength it is important to address the issue of the time of computation. Moreover, convergence is typically harder to achieve for objects with a large relative permittivity. In this article we first propose an algorithm that increases drastically the speed of the computation of optical forces. We also discuss recent formulations of the CDM that improve the accuracy of the calculation of optical forces for objects with a large relative permittivity.

In Sec. II we present the derivation of the optical forces. First, in Sec. II A, we recall the standard derivation of the force in the CDM and second, in Sec. II B, we show how the speed of the computation can be improved using fast-

Fourier-transform (FFT) techniques. In Sec. II C we focus on objects with a large relative permittivity. Numerical results are presented in Sec. III. We conclude in Sec. IV.

## II. THEORY

### A. Optical forces computed with the CDM

We start by recalling briefly the principle of the CDM [7]. The object under study is represented by a three-dimensional cubic array of  $N$  polarizable subunits. The electric field at each subunit position is derived from the self-consistent equation

$$\mathbf{E}(\mathbf{r}_i) = \mathbf{E}_0(\mathbf{r}_i) + \sum_{j=1, j \neq i}^N \mathbf{T}(\mathbf{r}_i, \mathbf{r}_j) \mathbf{p}(\mathbf{r}_j), \quad (1)$$

where  $\mathbf{E}_0(\mathbf{r}_i)$  is the incident field,  $\mathbf{E}(\mathbf{r}_i)$  is the local field at position  $\mathbf{r}_i$ , and  $\mathbf{p}(\mathbf{r}_j) = \alpha(\mathbf{r}_j) \mathbf{E}(\mathbf{r}_j)$  is the dipole moment of subunit  $j$ .  $\mathbf{T}$  is the linear response of the electric field to a dipole in free space [8]. Notice that the term  $\mathbf{T}(\mathbf{r}_i, \mathbf{r}_j) = -(4\pi/3) \mathbf{I} \delta(\mathbf{r}_i - \mathbf{r}_j)$ , where  $\mathbf{I}$  is the unit tensor, is taken into account in the polarizability through the Clausius-Mossotti relation [8,9].  $\alpha(\mathbf{r}_j)$  is the dynamic polarizability of subunit  $j$ ; it includes the radiation reaction term that is required to satisfy the optical theorem and which cannot be neglected in the computation of optical forces [10]:

$$\alpha_0(\mathbf{r}_i) = \frac{3d^3 \varepsilon(\mathbf{r}_i) - 1}{4\pi \varepsilon(\mathbf{r}_i) + 2}, \quad (2)$$

$$\alpha(\mathbf{r}_i) = [1 - (2/3)ik^3 \alpha_0(\mathbf{r}_i)]^{-1} \alpha_0(\mathbf{r}_i), \quad (3)$$

where  $d$  is the period of the discretization lattice,  $\varepsilon$  the relative permittivity of the object, and  $k$  the wave number. No-

tice that Eqs. (2) and (3) hold for a tensorial polarizability. Once the local electric field is known through Eq. (1), the time average of the optical force acting on each subunit is obtained as

$$F_u(\mathbf{r}_i) = (1/2)\text{Re}\left(\sum_{v=1}^3 p_v(\mathbf{r}_i) \frac{\partial(E_v(\mathbf{r}_i))^*}{\partial u}\right), \quad (4)$$

where  $u$  and  $v$  stand for either  $x$ ,  $y$ , or  $z$ . The symbol  $*$  denotes the complex conjugate. The derivative of the electric field, i.e.,  $\partial(E_v(\mathbf{r}_i))^*/\partial u$ , is given by

$$\left(\frac{\partial\mathbf{E}(\mathbf{r})}{\partial u}\right)_{\mathbf{r}=\mathbf{r}_i} = \left(\frac{\partial\mathbf{E}_0(\mathbf{r})}{\partial u}\right)_{\mathbf{r}=\mathbf{r}_i} + \sum_{j=1, j\neq i}^N \left(\frac{\partial}{\partial u}\mathbf{T}(\mathbf{r}, \mathbf{r}_j)\right)_{\mathbf{r}=\mathbf{r}_i} \mathbf{p}(\mathbf{r}_j). \quad (5)$$

The detailed derivation of Eq. (5) is given in the Appendix. As one can see, the derivative of the local field at  $\mathbf{r}_i$ , requires the knowledge of the derivative of  $\mathbf{E}_0(\mathbf{r}_i)$  and of  $\mathbf{T}(\mathbf{r}_i, \mathbf{r}_j)$  for all  $i$  and  $j$ .

The net optical force on the object is obtained as the sum over all the subunits of the individual forces:

$$\mathbf{F} = \sum_{i=1}^N \mathbf{F}(\mathbf{r}_i). \quad (6)$$

The method presented above has been described extensively in previous articles (see for example Ref. [6]), and we will call this method the RRCDM: The CDM with the radiation reaction term included in the polarizability.

## B. Improving the speed of the computation of optical forces

The drawback of the previous method is that the computation time of the optical force becomes prohibitive for large  $N$ . The computation time pertains mostly to the computation of the derivative of the electric field, i.e., Eq. (5). For the sake of convenience we can write Eq. (5) in a symbolic form:

$$\partial_u \mathbf{E}(\mathbf{r}_i) = \partial_u \mathbf{E}_0(\mathbf{r}_i) + \sum_{j=1, j\neq i}^N [\partial_u \mathbf{T}(\mathbf{r}_i, \mathbf{r}_j)] \mathbf{p}(\mathbf{r}_j) \quad (7)$$

with  $u=x, y$ , or  $z$ . We now describe a strategy that reduces drastically the time of computation of Eq. (7). First we use the fact that  $\partial_u \mathbf{T}(\mathbf{r}_i, \mathbf{r}_j)$  depends only on the difference of the position vectors  $\mathbf{r}_i - \mathbf{r}_j$ . Consider a discretization box with dimensions  $N_x d$ ,  $N_y d$ , and  $N_z d$  which contains the scattering object. We define the polarizability over the box as  $\alpha_{i_x, i_y, i_z}(\mathbf{r}_{i_x, i_y, i_z})=0$  for a subunit lying outside the object (note that  $i_x=1, \dots, N_x$ ,  $i_y=1, \dots, N_y$ , and  $i_z=1, \dots, N_z$ ), and  $\alpha_{i_x, i_y, i_z}(\mathbf{r}_{i_x, i_y, i_z})=\alpha(\mathbf{r}_i)$  otherwise. We now double the size of the lattice in each dimension and treat all quantities as periodic in three dimensions with periods  $2N_x$ ,  $2N_y$ , and  $2N_z$ . Note that the actual object is neither doubled in size, nor made periodic. This is merely a numerical technique that allows us to treat the convolution product as a cyclic convolution. The matrix containing the derivatives of the field susceptibility is Toeplitz, i.e., each of its elements can be labeled by  $i-j$  instead of  $(i, j)$ . To use FFTs we need to embed the

Toeplitz matrix into a circulant matrix of twice the size whose element  $-i$  is equal to element  $K-i$  for  $0 \leq i \leq K-1$ , and where  $K$  is the order of the circulant matrix (twice the order of the original matrix). The matrix-vector convolution product can now be computed by FFT after the vector is doubled in size and padded with zeros. The result of the original convolution product is then obtained by cropping the result of the cyclic convolution down to the size of the original vector. Hence, omitting the derivative of the incident field, we can rewrite Eq. (7) as

$$\mathbf{Y}_{i_x, i_y, i_z} = \sum_{j_x=1}^{2N_x} \sum_{j_y=1}^{2N_y} \sum_{j_z=1}^{2N_z} [\partial_u \mathbf{T}(\mathbf{r}_{i_x, i_y, i_z} - \mathbf{r}_{j_x, j_y, j_z})] \mathbf{X}(\mathbf{r}_{j_x, j_y, j_z}) \quad (8)$$

with  $\mathbf{X}(\mathbf{r}_{j_x, j_y, j_z}) = \mathbf{p}(\mathbf{r}_{j_x, j_y, j_z})$  for  $j_x \leq N_x$  and  $j_y \leq N_y$  and  $j_z \leq N_z$ , and  $\mathbf{X}(\mathbf{r}_{j_x, j_y, j_z}) = \mathbf{0}$  everywhere else. Notice that we also take  $\partial_u \mathbf{T}(\mathbf{r}_{i_x, i_y, i_z} - \mathbf{r}_{i_x, i_y, i_z}) = \mathbf{0}$ . It is now obvious that Eq. (8) is a convolution product which can be computed in a very efficient way using a FFT [11]. For any given value of  $u$  we treat each component  $x$ ,  $y$ , and  $z$  separately. As  $\mathbf{X}(\mathbf{r}_{j_x, j_y, j_z})$  is not a derivative, it needs only three FFTs (one for each component). On the other hand,  $\partial_u \mathbf{T}$  requires 27 FFTs due to the fact that each component of the linear field tensor susceptibility is differentiated along  $x$ ,  $y$ , and  $z$ . In fact, owing to the symmetry of the derivative of the tensor one needs to compute only 18 FFTs. Once the products of the FFTs of  $\mathbf{X}$  and  $\partial_u \mathbf{T}$  are computed, one can obtain  $\mathbf{Y}$  by inverse FFT. As shown in Eq. (7), one needs to add the derivative of the incident field to get the derivative of the local field.

## C. Improving the accuracy of the computation of the optical forces for scatterers with large relative permittivity

### 1. Homogeneous ellipsoid

The objects manipulated in optical force experiments are often homogeneous spheres or ellipsoids [5]. For such shapes it is possible to improve drastically the accuracy of the CDM [12]. The idea is based on the fact that the polarizability of each subunit depends on its environment, i.e., the polarizability is not the same for a subunit at the center of the object and one at its edge.

We recall briefly here the derivation of this polarizability which takes into account the variation of the local field over the volume of the scatterer [12]. We begin by making the static approximation, i.e.,  $k=0$ , and assuming the object is embedded in a uniform applied field  $\mathbf{E}_{\text{app}}$ . In this case the macroscopic field  $\mathbf{E}_{\text{mac}}$  inside the object can be written as

$$\left(\mathbf{I} + \frac{\varepsilon - 1}{4\pi} \mathbf{L}\right) \mathbf{E}_{\text{mac}} = \mathbf{E}_{\text{app}} \quad (9)$$

where  $\mathbf{L}$  is the depolarization tensor. Then, with the help of Eq. (9), Eq. (1) can be written

$$\mathbf{E}_s(\mathbf{r}_i) = \left(\mathbf{I} + \frac{\varepsilon - 1}{4\pi} \mathbf{L}\right) \mathbf{E}_{\text{mac}} + \sum_{j=1, j\neq i}^N \mathbf{T}_s(\mathbf{r}_i, \mathbf{r}_j) \alpha_s(\mathbf{r}_j) \mathbf{E}_s(\mathbf{r}_j). \quad (10)$$

The subscript  $s$  recalls that we are in the static case. Notice that in Eq. (10) the polarizability is a tensor. In using the

well-known relations between the polarization, the local field, and the macroscopic field, the static polarizability can be written as

$$\alpha_s(\mathbf{r}_i) = \frac{\varepsilon(\mathbf{r}_i) - 1}{4\pi} d^3 \times \left[ \mathbf{I} + \frac{\varepsilon(\mathbf{r}_i) - 1}{4\pi} \left( \mathbf{L} + d^3 \sum_{j=1}^N \mathbf{T}_s(\mathbf{r}_i, \mathbf{r}_j) \right) \right]^{-1}. \quad (11)$$

For example, for a homogeneous sphere the depolarization factor is  $\mathbf{L} = (4\pi/3)\mathbf{I}$  [13]. Note that if  $\sum_{j=1}^N \mathbf{T}_s(\mathbf{r}_i, \mathbf{r}_j) = 0$ , one finds the usual Clausius-Mossotti relation. The depolarization factor for an ellipsoid can be found in Ref. [14]. Notice that this polarizability is defined in the static case. Therefore, to compute optical forces one should add the radiation reaction term and introduce  $\alpha_s$  inside Eq. (3) instead of  $\alpha_0$ .

We emphasize that this method to improve the precision of the local field is limited to homogeneous objects which have a constant depolarization factor. We will call this method the local-field-corrected CDM (LFCCDM).

## 2. Arbitrary object

For an arbitrary object with a large relative permittivity (a case where the RRCM fails) one can improve the performance of CDM through volume integration. This approach is more computationally involved than the one presented in Sec. II C 1. When we write Eq. (1) we make the assumption that the free-space tensor field susceptibility  $\mathbf{T}$  is uniform over the size of the subunit. If we want to take into account the variation of  $\mathbf{T}$  over the subunit, we should write Eq. (1) in the integral form [9]

$$\mathbf{E}_{\text{ins}}(\mathbf{r}) = \mathbf{E}_0(\mathbf{r}) + \int_V \mathbf{T}(\mathbf{r}, \mathbf{r}') \chi(\mathbf{r}') \mathbf{E}_{\text{ins}}(\mathbf{r}') d\mathbf{r}', \quad (12)$$

where the integration is performed over the volume of the object, and  $\mathbf{E}_{\text{ins}}$  is the macroscopic field inside the object.  $\chi(\mathbf{r}')$  is the linear susceptibility of the object. We discretize the scatterer in  $N$  subunits as done previously, and we assume the linear susceptibility is uniform over each subunit:

$$\mathbf{E}_{\text{ins}}(\mathbf{r}) = \mathbf{E}_0(\mathbf{r}) + \sum_{j=1}^N \int_{V_j} \mathbf{T}(\mathbf{r}, \mathbf{r}') \chi(\mathbf{r}_j) \mathbf{E}_{\text{ins}}(\mathbf{r}') d\mathbf{r}'. \quad (13)$$

If the variation of the macroscopic field in each subunit is small enough, we have  $\mathbf{E}_{\text{ins}}(\mathbf{r}') \approx \mathbf{E}_{\text{ins}}(\mathbf{r}_j)$  on the subunit  $j$ . Then after some tedious calculation, Eq. (13) can be expressed in terms of the local field as [9]

$$\mathbf{E}(\mathbf{r}_i) = \mathbf{E}_0(\mathbf{r}_i) + \sum_{j=1, j \neq i}^N \frac{\mathbf{T}^{\text{int}}(\mathbf{r}_i, \mathbf{r}_j)}{V_j} \alpha^{\text{int}}(\mathbf{r}_j) \mathbf{E}(\mathbf{r}_j), \quad (14)$$

where the polarizability of the subunit  $j$  is now expressed as

$$\alpha^{\text{int}}(\mathbf{r}_j) = \alpha_0(\mathbf{r}_j) \left( 1 - \frac{[\mathbf{T}^{\text{int}}(\mathbf{r}_j, \mathbf{r}_j) + 4\pi/3] \alpha_0(\mathbf{r}_j)}{V_j} \right)^{-1}. \quad (15)$$

$\mathbf{T}^{\text{int}}(\mathbf{r}_i, \mathbf{r}_j)$  represents the integral of the free-space field susceptibility tensor over the cubic subunit  $j$  (notice that La-

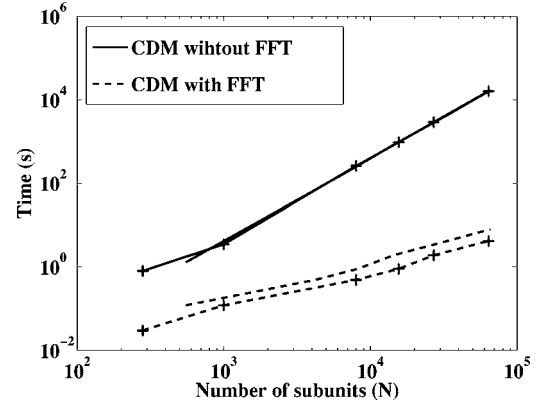


FIG. 1. Computation time in seconds versus the number of dipoles  $N$ . Solid lines: the derivatives are computed with the conventional CDM. Dashed lines: the derivative are computed using the FFT. Curves with crosses pertain to a cube, and the curves without any symbol pertain to a sphere.

htakia defines the polarizability by integrating the field susceptibility over a spherical region of the same volume as the cubic subunit [15]; in that case the polarizability is analytical). Once we know the local field at the positions of all the subunits, we can compute the optical forces using Eqs. (4)–(6). This integral form of the field susceptibility tensor (INTCDM) leads to an improved accuracy in the computation of the local field.

## III. RESULTS

### A. Computation time for the optical forces

We first investigate the computation time of the calculation of the optical forces from the knowledge of the self consistent local field at all the subunits. This is the time required to solve Eqs. (4)–(6). We perform this computation with the CDM as presented in Sec. II A and with the FFT method introduced in Sec. II B. Figure 1 shows the computation time for the derivative of the local field needed by the computation of the optical force. The computation is made on a personal computer with a 3 GHz processor. We consider different values of  $N$  and different shapes of the object. Results pertaining to a computation using the FFT method are in dashed lines, whereas the results of the conventional CDM computation (no FFT) are in solid lines. First, in the case of a cubic scatterer (lines with crosses) one can see that the FFT method reduces drastically the computation time. For example for  $N=64\,000$  the CDM with the FFT is  $10^4$  faster than the conventional CDM. The second case we consider is that of a spherical scatterer (Fig. 1, curves without symbols). As we mentioned in the previous section, the FFT requires the object to be placed within a rectangular domain. This implies that  $N < N_x \times N_y \times N_z$ ; hence the FFT method involves a larger number of dipoles than the conventional CDM (more or less twice as many in the case of a spherical scatterer). For the conventional CDM, the curves are superimposed for the two shapes. This is logical as the time of computation depends only on  $N$  and not on the shape of the object. For the CDM with the FFT, for a given volume of the

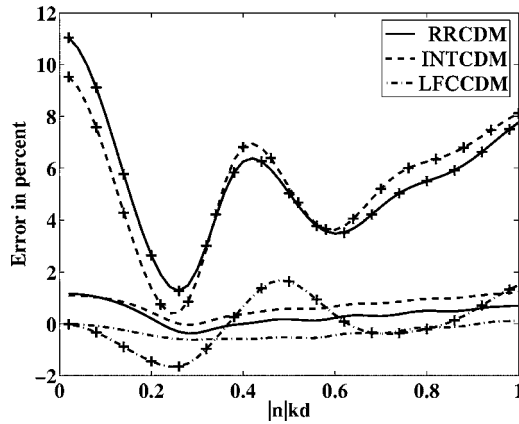


FIG. 2. Error in percent between the optical force compared to the Mie result for RRCDM (solid line), INTCDM (dashed line), and LFCCDM (dot-dashed line) versus  $|n|kd$ . Curves without symbol,  $\varepsilon=2.25+i$ ; curves with crosses,  $\varepsilon=10+10i$ .

scatterer (i.e., a given  $N$ ), the computation time is longer for a sphere than for a cube because of the extra dipoles that are needed to place the sphere into a rectangular domain. But despite this increase in the number of dipoles it is easy to see that it is always faster to use the CDM with the FFT.

### B. Scatterers with large relative permittivity

In the previous section we have shown how the use of FFT can improve dramatically the speed of the calculation of optical forces. Now we tackle the task of improving the accuracy of the computation of optical forces using the CDM. To estimate the accuracy of the different computational methods presented in this article we consider the scattering by a homogeneous sphere illuminated by a plane wave. In this configuration we can compare our results to the exact solution:

$$\mathbf{F}_{\text{Mie}} = \frac{1}{8\pi} |\mathbf{E}_0|^2 (C_{\text{ext}} - \overline{\cos \theta} C_{\text{sca}}) \frac{\mathbf{k}}{k} \quad (16)$$

where  $C_{\text{ext}}$  denotes the extinction cross section,  $C_{\text{sca}}$  the scattering cross section, and  $\overline{\cos \theta}$  the average of the cosine of the scattering angle.  $C_{\text{ext}}$ ,  $C_{\text{sca}}$ , and  $\overline{\cos \theta}$  can be computed as Mie series. We compare the optical force obtained with the Mie calculation to the force computed with the RRCDM, the LFCCDM, and the INTCDM. In all calculations FFT techniques are used to accelerate the computation of the fields and their derivatives.

Figure 2 shows the relative error in percent between the optical force computed with the Mie series, and the other three methods presented in this article. The force is plotted versus  $|n|kd$  ( $n=\sqrt{\varepsilon}$ ) for  $\varepsilon=2.25+i$  and a larger relative permittivity:  $\varepsilon=10+10i$ . It is obvious that the local field correction introduced in the polarizability (LFCCDM) yields the best results. The advantage of this method is also that when  $d$  decreases the error vanishes. This is not the case for the other two methods. For  $\varepsilon=2.25+i$  the RRCDM result and the INTCDM result are very close. For small  $d$  the INTCDM is slightly better but the error becomes a little larger than for

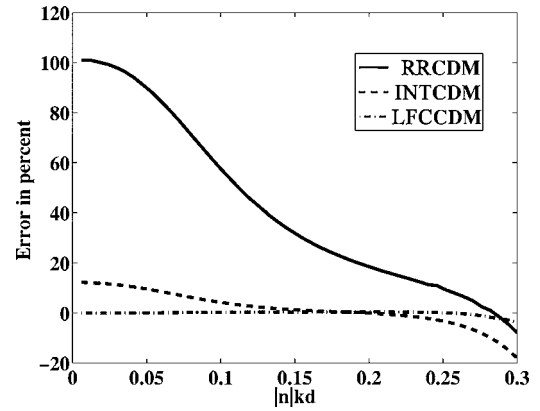


FIG. 3. Same as Fig. 2 but for  $\varepsilon=25+i$ .

RRCDM when  $d$  increases. This is easy to understand, when the subunit is small compared to the wavelength the approximation of a uniform field inside the subunit [Eq. (13)] is valid and thus the integration of the tensor improves the accuracy of the estimate of the local field.

For  $\varepsilon=10+10i$ , the INTCDM is better than the RRCDM up to  $|n|kd=0.25$ . This is due to the fact that for a fixed value of  $|n|kd$ ,  $d$  is smaller when  $\varepsilon=10+10i$  than when  $\varepsilon=2.25+i$ , hence the INTCDM converges better. We now consider a larger permittivity:  $\varepsilon=25+i$ . Beyond  $|n|kd=0.3$  all the methods fail to yield an accurate result. However, one can see in Fig. 3 that for smaller values of  $|n|kd$  the RRCDM yields the wrong result whereas the INTCDM result is always less than 20% away from the correct result, and the LFCCDM result is always less than 5% away from the correct result. Notice that  $|n|kd=0.3$  gives in that case  $d=0.02\lambda$ . The spacing is very small compared to the wavelength in vacuum, due to the large value of the relative permittivity.

To be more general, Fig. 4 shows the relative error in percent on the optical force for a given value  $|n|kd=0.02$ , versus the real part of the relative permittivity. This is done for the three different methods, and different values of the

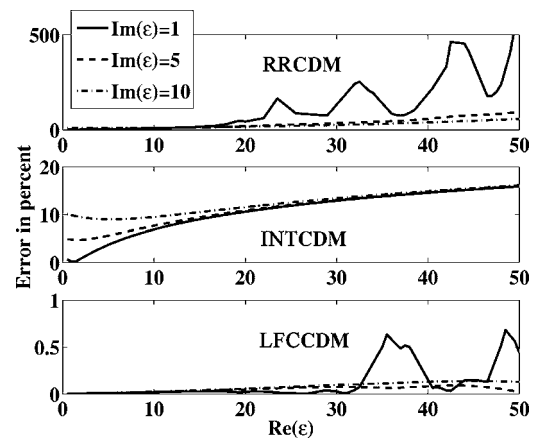


FIG. 4. Error in percent between the optical force obtained from the Mie series and the RRCDM (top), INTCDM (middle), and LFCCDM (bottom) versus  $\text{Re}(\varepsilon)$  with  $|n|kd=0.02$ . In solid lines,  $\text{Im}(\varepsilon)=1$ ; in dashed lines,  $\text{Im}(\varepsilon)=5$ ; and in dot-dashed lines,  $\text{Im}(\varepsilon)=10$ .

imaginary part of the relative permittivity. Figure 4(a) pertains to the RRCDM, Fig. 4(b) to the INTCDM, and Fig. 4(c) to the LFCCDM. In Fig. 4(a) it is obvious that the error on the optical force is dramatic, and that decreasing the imaginary part of the relative permittivity worsens the accuracy of the calculation. This is due to the presence of morphological resonance inside the sphere which are damped if the imaginary part of the relative permittivity is large enough. The INTCDM gives an error always below 17% irrespective of the value of the relative permittivity. The results are correct for small value of  $d$  with these very large relative permittivity. But the LFCCDM gives an error always below 1% and this for all the values of the relative permittivity even in the presence of the morphological resonances.

#### IV. CONCLUSIONS

In conclusion we showed how the computation of optical forces with the CDM can be drastically improved by using FFT techniques to calculate convolution products. We also addressed the issue of objects with a large relative permittivity. The best results are obtained when local-field corrections are included in the formulation of the polarizabilities used in the CDM. However, this formulation can be only be used with objects that have a uniform depolarization tensor. Incidentally such objects (spheres or ellipsoids) are often used in experiments. For a general, arbitrary object, we showed that the accuracy of the CDM can be improved through the integration of the field susceptibility over each subunit.

#### ACKNOWLEDGMENT

A.R. acknowledges financial support from the Ministère délégué à la Recherche et aux Nouvelles Technologies (Program "ACI Jeune Chercheur").

#### APPENDIX: DERIVATIVE OF THE LOCAL FIELD

To derive Eq. (5) we start from the volume-integral equation, i.e., Eq. (13). We take the derivative of Eq. (13) at  $\mathbf{r}$ :

$$\partial_u \mathbf{E}_{\text{ins}}(\mathbf{r}) = \partial_u \mathbf{E}_0(\mathbf{r}) + \sum_{j=1}^N \int_{V_j} [\partial_u \mathbf{T}(\mathbf{r}, \mathbf{r}')] \chi(\mathbf{r}_j) \mathbf{E}_{\text{ins}}(\mathbf{r}') d\mathbf{r}'. \quad (\text{A1})$$

We then write Eq. (A1) for  $\mathbf{r}=\mathbf{r}_i$  and we separate in the sum the case  $i=j$ :

$$\begin{aligned} \partial_u \mathbf{E}_{\text{ins}}(\mathbf{r}_i) &= \partial_u \mathbf{E}_0(\mathbf{r}_i) + \sum_{j=1, j \neq i}^N \int_{V_j} [\partial_u \mathbf{T}(\mathbf{r}_i, \mathbf{r}')] \chi(\mathbf{r}_j) \mathbf{E}_{\text{ins}}(\mathbf{r}') d\mathbf{r}' \\ &+ \int_{V_i} [\partial_u \mathbf{T}(\mathbf{r}_i, \mathbf{r}')] \chi(\mathbf{r}_i) \mathbf{E}_{\text{ins}}(\mathbf{r}') d\mathbf{r}'. \end{aligned} \quad (\text{A2})$$

Using the symmetry property of the tensor  $\partial_u \mathbf{T}(\mathbf{r}_i, \mathbf{r}')$

$= -\partial_u \mathbf{T}(\mathbf{r}_i, \mathbf{r}')$ , the last term of Eq. (A2) can be written as

$$\begin{aligned} &\int_{V_i} [\partial_u \mathbf{T}(\mathbf{r}_i, \mathbf{r}')] \chi(\mathbf{r}_i) \mathbf{E}_{\text{ins}}(\mathbf{r}') d\mathbf{r}' \\ &= - \int_{V_i} \partial_u [\mathbf{T}(\mathbf{r}_i, \mathbf{r}') \chi(\mathbf{r}_i) \mathbf{E}_{\text{ins}}(\mathbf{r}')] d\mathbf{r}' \\ &+ \int_{V_i} \mathbf{T}(\mathbf{r}_i, \mathbf{r}') \chi(\mathbf{r}_i) \partial_u [\mathbf{E}_{\text{ins}}(\mathbf{r}')] d\mathbf{r}'. \end{aligned} \quad (\text{A3})$$

Assuming that  $\mathbf{E}_{\text{ins}}(\mathbf{r}')$  varies linearly with respect to  $x'$ ,  $y'$ , and  $z'$  over the subunit  $i$ , we find  $\int_{V_i} \partial_u [\mathbf{T}(\mathbf{r}_i, \mathbf{r}') \chi(\mathbf{r}_i) \mathbf{E}_{\text{ins}}(\mathbf{r}')] d\mathbf{r}' = 0$  and that  $\partial_u [\mathbf{E}_{\text{ins}}(\mathbf{r}')] is a constant. Then Eq. (A3), assuming the volume  $V_i$  is very small compared to the wavelength [9], reduces to$

$$\begin{aligned} &\int_{V_i} [\partial_u \mathbf{T}(\mathbf{r}_i, \mathbf{r}')] \chi(\mathbf{r}_i) \mathbf{E}_{\text{ins}}(\mathbf{r}') d\mathbf{r}' \\ &= \chi(\mathbf{r}_i) \partial_u \mathbf{E}_{\text{ins}}(\mathbf{r}_i) \int_{V_i} \mathbf{T}(\mathbf{r}_i, \mathbf{r}') d\mathbf{r}' \\ &= - \frac{4\pi}{3} \chi(\mathbf{r}_i) \partial_u \mathbf{E}_{\text{ins}}(\mathbf{r}_i). \end{aligned} \quad (\text{A4})$$

Hence using Eq. (A4) and assuming the field-susceptibility tensor constant over a subunit, Eq. (A2) can be written as

$$\begin{aligned} &\partial_u \left( \mathbf{E}_{\text{ins}}(\mathbf{r}_i) \frac{\varepsilon(\mathbf{r}_i) + 2}{3} \right) \\ &= \partial_u \mathbf{E}_0(\mathbf{r}_i) + \sum_{j=1, j \neq i}^N \partial_u \mathbf{T}(\mathbf{r}_i, \mathbf{r}_j) \chi(\mathbf{r}_j) V_j \mathbf{E}_{\text{ins}}(\mathbf{r}_j) \\ &= \partial_u \mathbf{E}_0(\mathbf{r}_i) + \sum_{j=1, j \neq i}^N \\ &\quad \times \partial_u \mathbf{T}(\mathbf{r}_i, \mathbf{r}_j) \frac{3d^3 \varepsilon(\mathbf{r}_j) - 1}{4\pi \varepsilon(\mathbf{r}_j) + 2} \frac{\varepsilon(\mathbf{r}_j) + 2}{3} \mathbf{E}_{\text{ins}}(\mathbf{r}_j). \end{aligned} \quad (\text{A5})$$

In Eq. (A5) we recognize the polarizability  $\alpha_0(\mathbf{r}_j)$  along with the local field  $\mathbf{E}(\mathbf{r}_j) = \mathbf{E}_{\text{ins}}(\mathbf{r}_j) [\varepsilon(\mathbf{r}_j) + 2]/3$ . Notice that in Eq. (A5) the polarizability is different from the one defined in Eq. (3). This is due to the fact that for the sake of simplicity we have approximated  $\int_{V_i} \mathbf{T}(\mathbf{r}_i, \mathbf{r}') d\mathbf{r}'$  to  $-4\pi/3$ ; in fact performing the integration rigorously yields the radiation reaction term in the polarizability [9].

- [1] M. J. Lang and S. M. Block, *Am. J. Phys.* **71**, 201 (2003).
- [2] S. Mancini, V. Giovannetti, D. Vitali, and P. Tombesi, *Phys. Rev. Lett.* **88**, 120401 (2002); W. Marshall, C. Simon, R. Penrose, and D. Bouwmeester, *ibid.* **91**, 130401 (2003).
- [3] L. Novotny, R. X. Bian, and X. S. Xie, *Phys. Rev. Lett.* **79**, 645 (1997).
- [4] K. Okamoto and S. Kawata, *Phys. Rev. Lett.* **83**, 4534 (1999).
- [5] A. I. Bishop, T. A. Nieminen, N. R. Heckenberg, and H. Rubinsztein-Dunlop, *Phys. Rev. A* **68**, 033802 (2003).
- [6] P. C. Chaumet and M. Nieto-Vesperinas, *Phys. Rev. B* **64**, 035422 (2001); **62**, 11185 (2000); **61**, 14119 (2000).
- [7] E. M. Purcell and C. R. Pennypacker, *Astrophys. J.* **186**, 705 (1973).
- [8] J. D. Jackson, *Classical Electrodynamics*, 2nd ed. (John Wiley, New York, 1975).
- [9] P. C. Chaumet, A. Sentenac, and A. Rahmani, *Phys. Rev. E* **70**, 036606 (2004).
- [10] P. C. Chaumet and M. Nieto-Vesperinas, *Opt. Lett.* **25**, 1065 (2000).
- [11] J. J. Goodman, B. T. Draine, and P. J. Flatau, *Opt. Lett.* **16**, 1198 (2001).
- [12] A. Rahmani, P. C. Chaumet, and G. W. Bryant, *Astrophys. J.* **607**, 873 (2004); *Opt. Lett.* **27**, 2118 (2002).
- [13] A. D. Yaghjian, *Proc. IEEE* **68**, 248 (1980).
- [14] J. A. Stratton, *Electromagnetic Theory* (McGraw-Hill, New York, 1941).
- [15] A. Lakhtakia and G. Mulholland, *J. Res. Natl. Inst. Stand. Technol.* **98**, 699 (1993); A. Lakhtakia, *Int. J. Mod. Phys. C* **3**, 583 (1992).